Phys. Status Solidi C **7**, No. 11–12, 2628–2631 (2010) / **DOI** 10.1002/pssc.200983826

physica status solidi c
www.pss-c.com
current topics in solid state physics

Mobility gaps in disordered graphene-based materials: an *ab initio*-based tight-binding approach to mesoscopic transport

Blanca Biel[*,1], Alessandro Cresti[2], Rémi Avriller[3], Simon Dubois[4], Alejandro López-Bezanilla[5], François Triozon[2], X. Blase[6], Jean-Christophe Charlier[4], and Stephan Roche[7,8]

[1] Dpto. Electrónica y Tecnología de Computadores, Facultad de Ciencias, and CITIC, Universidad de Granada, 18071 Granada, Spain
[2] CEA, LETI, MINATEC, 38054 Grenoble, France
[3] Departamento de Física Teórica de la Materia Condensada C-V, Facultad de Ciencias, Universidad Autónoma de Madrid, 28049 Madrid, Spain
[4] PCPM & ETSF, Université Catholique de Louvain, Place Croix du Sud, 1 B-1348 Louvain-la-Neuve, Belgique
[5] CEA, INAC, SPSMS, 17 rue des Martyrs, 38054 Grenoble Cedex 9, France
[6] Institut Néel, CNRS and Université Joseph Fourier, B.P. 166, 38042 Grenoble Cedex 9, France
[7] CIN2 (CSIC-ICN), Campus UAB, 08193 Barcelona, Spain
[8] CEA, INAC, SP2M, $L_{\rm sim}$, 17 avenue des Martyrs, 38054 Grenoble, France

Received 16 October 2009, revised 19 January 2010, accepted 19 January 2010
Published online 9 August 2010

Keywords: graphene, nanoribbons, carbon nanotubes, doping, electronic transport, electronic structure calculations

* Corresponding author: e-mail Biel@ugr.es

As is common knowledge, armchair graphene nanoribbons (aGNRs) share many electronic features with carbon nanotubes (CNTs). Nevertheless, crucial differences emerge when disorder comes into play. It is thus instructive, both from a theoretical and a technological perspective, to analyze the impact of possible types of disorder on the transport properties of these graphene-based materials.
Here we report such a comparative study between CNTs and GNRs, which points out the similarities and differences emerging as a consequence of doping by substitutional boron and nitrogen impurities. The role of edge defects (absent in CNTs) is also contrasted with chemical doping disorder. All disorder models have been derived from accurate *ab initio* calculations of the electronic structures.

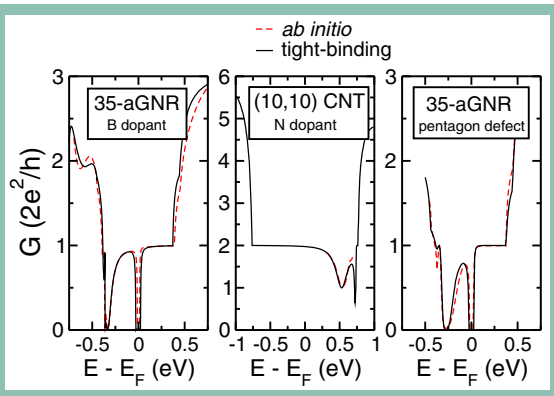

Conductance as a function of the energy for the (left) single boron dopant, (center) nitrogen dopant, (left) edge defect case, for a 35-aGNR (left and right) and for a (10,10) CNT (center). Red dashed curves: Results for the fully *ab initio* Hamiltonian. Black solid lines: Results for the tight-binding Hamiltonian with the tuned parametrization (see text).

1 Introduction The understanding of transport properties in disordered and chemically modified graphene-based materials has become a main issue of concern in view of their use in the future carbon-based nanoelectron-

ics. Quantum transport in CNTs and GNRs was recently reviewed [1,2]. Disorder strongly impacts transport properties in low dimensional systems, but it turns out that in carbon-based materials it could be also used to obtain new device functionalities (sensing, memories, NEMS, ...) or to upscale device performances. Especially, chemically doped GNRs have been recently shown [3] to develop transport gaps as large as 1 eV as a consequence of strong impurity-induced electron-hole asymmetrical backscattering phenomena [4]. Although ribbons share a similar underlying electronic structure with CNTs, their response to certain types of disorder might lead to considerable differences in their transport properties [2].

In this letter we report a mesoscopic transport study of two similar systems: an armchair (metallic) (10,10) CNT, and an armchair GNR [5] (which presents a small gap [6]). We analyze transport regimes through the extraction of the main transport length scales (mean free paths and localization lengths) and show the highest robustness of CNTs against disorder. The effect of chemical impurities in CNTs and GNRs is also compared with the impact of edge disorder (missing atoms at the edges) unique to ribbons.

2 Disorder models Both the chemical doping and the edge disorder models have been obtained from *ab initio* calculations of the electronic structure for each considered graphene-based system. The SIESTA package [7] was used for this purpose (simulation details can be found in refs. [4,8,9].) A fine tight-binding (TB) parametrization has been extracted in each case in order to reproduce the first-principles results for the conductance profile of the single-defect system (see abstract figure). The TB Hamiltonian is then used to perform mesoscopic transport calculations, which provide some estimation on the magnitude of the mobility gaps and the typical transport lengths.

Substitutional doping In the case of boron (nitrogen) impurities, an *ab initio* Density Functional Theory (DFT)-based study is first performed for the infinite armchair GNR (CNT) when one of the carbon atoms is substituted by a boron [4] (nitrogen [8]) dopant. The self-consistent calculation provides the behaviour of the scattering potential around the impurity. In a second step, the onsite and hopping self-consistent Hamiltonian matrix elements (on a localized basis set) are used to build the TB Hamiltonian. This technique [10] has been successfully employed in the study of the electronic properties in carbon systems at the mesoscopic scale [8,11,3], since it combines the accuracy of *ab initio* calculations with the low computational cost allowed by a TB Hamiltonian (see abstract figure).

Edge disorder The edge disorder model is elaborated in a similar way. The nearest-neighbor TB Hamiltonian is appropriately tuned in order to reproduce the conductance profile for a single defect in an infinite GNR [10,9] (see abstract figure). Mesoscopic transport calculations are then performed using this Hamiltonian.

3 GNRs vs. CNTs We have chosen to compare an armchair (10,10) CNT [1] to an armchair 35-aGNR, with 35 dimer lines across the ribbon width. The circumference of the CNT ($\approx$ 4.2 nm) is very similar to the width of the ribbon ($\approx$ 4.4 nm) and the electronic structure of both systems show a resemblance with the linear dispersion of bands at the Fermi level of 2D-graphene. In the case of (10,10) CNTs, the system is metallic and the bands cross at the K point of the Brillouin zone. The armchair nanoribbon is semiconducting [6], but its energy gap is very small ($\approx$ 0.03 eV), as in the case of other N-aGNR with N=3p+2, where p is an integer number. The comparison, then, between the (10,10) CNT and the 35-aGNR seems very reasonable, at least from a qualitatively perspective, to extract some general features about the response to chemical doping in both systems.

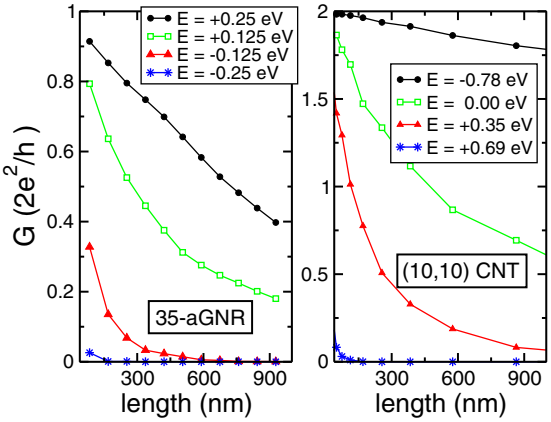

Figure 1 Conductance as a function of the length for the 35-aGNR (left) and the (10,10) CNT at a doping rate of 0.1% for several values of the energy E. The onset of the localization regime can be seen as E approaches the valence band.

3.1 Results for chemical doping Apart from their different acceptor and donor characters, boron and nitrogen doping share several similarities. The conductance profiles of boron doped CNTs (GNRs) turn out to be almost specular (with respect to the charge neutrality point) to those of nitrogen doped CNTs (GNRs) [12,4]. This makes possible a comparison between boron doped GNRs and nitrogen doped CNTs. Some of the results presented below for the CNTs have been partly discussed elsewhere [8,11]. In this work, we provide the first quantitative comparison of the effect of similar doping density on transport features of nanotubes and ribbons materials.

One important point to first notice is the absence of rotational symmetry in GNRs in contrast to CNTs. As a consequence, the conductance profile of CNTs with a single impurity does not depend on the position of the defect itself [13]. On the other hand, the position of the dopant with respect to the edges yields large conductance variations for GNRs [4]. As a result, large differences are expected to occur between the transport properties of the two doped ma-

terials, as discussed below. Although the unrolled nanotube and the armchair ribbons present a similar width, the onset of their conductance plateaus is a bit different. This makes impossible to use directly the same energy values used in Ref.[8] for the extraction of the mean free path l_e and the localization length ξ in the case of the GNR. For this reason, we have chosen for the 35-aGNR certain "equivalent" energies that are comparable (taking into account their position with respect to the van Hove singularities and their behaviour when disorder is introduced) to the ones studied for the (10,10) CNT.

As shown in Figs. 1 and 2, ribbons appear to be much more sensitive to the presence of chemical impurities than CNTs are. This is first seen by noting that, for the same doping rate of n_{dop} ≈0.1%, the quasiballistic regime in a 35-aGNR is more difficult to recover for any value of the energy than in the case of the CNT, where l_e of several microns are obtained. The estimated length for the l_e is actually one order of magnitude smaller for the GNR. This is partly due to the existence of a single transport channel for GNR, which enhances the tendency towards strong localization.

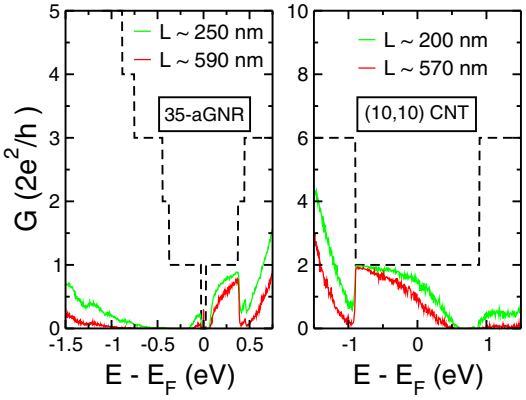

Figure 2 Conductance as a function of the energy for the 35-aGNR (left) and the (10,10) CNT (right) at a doping rate of 0.1% for several fixed lengths. The onset of the mobility gaps is clearly seen even for those short lengths.

4 Doping vs. edge disorder The issue of edge disorder has attracted much attention from the graphene community (see, for instance,[14–18,9]). Edge defects are unavoidable in GNRs and they occur at both growth and patterning processes. Since their presence might affect the electronic and transport properties considerably, it is useful to explore the impact of possible edge defects, not only on the electronic structure of GNRs, but also on the transport scaling lengths. Up to date, most of the efforts on this topic have been done using a rather simplified topological TB model or a even more generic Anderson-like disorder model ([16]). *Ab initio* calculations have mainly concentrated on the possible geometrical reconstructions that take place at the edges when carbon atoms are removed [19]. The charge transfer between atoms observed for certain configurations determines the limits of the topological TB model, which is not able to include such an effect.

A more refined TB model has thus been developed in order to accurately describe the transport signature of isolated edge defects according to the *ab initio* calculations [9]. While the validity of the TB model has been presented elsewhere [9], here we pinpoint the main similarities and differences with respect to the chemical doping. Among the possible reconstructions, we have selected the pentagon-like edge defect, since its conductance profile reminds closely that of the boron impurity.

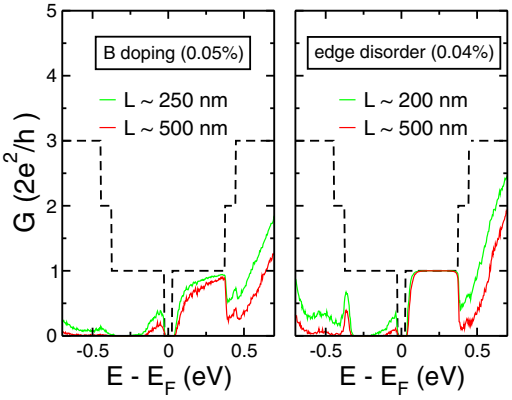

Figure 3 Conductance as a function of the energy for the 35-aGNR at a (left) doping rate of 0.05% and (right) edge defect density of 0.04% for several fixed lengths.

Figure 3 shows the conductance profile as a function of energy for a 35-aGNR in the case of boron doping (left panel) and pentagon-like defects (right panel). The conductance curves are averaged over 400 disorder configurations (i.e. different distributions of dopants or defects compatible with a (fixed) given doping rate or defect density). As can be seen in the plot, both types of disorder lead to the onset of mobility gaps in the valence band of the aGNR, although the boron doping seems more efficient and opens a larger gap for a similar length. This is a consequence of the wider distribution of quasibound states over the entire valence band in the first conductance plateau, due to the random distribution of dopants across the ribbon width and the strong dependence of the scattering potential with the dopant position with respect to the ribbon edge [4].

The conductance in the conduction band, although keeping high values for both disorder models, is better preserved in the case of this specific edge defect. The particular nature of the scattering potential, which induces quasi-bound states in the valence band while affecting very weakly the electronic states with energies above the charge neutrality point in the first conductance plateau [20], leads to a quasi-ballistic transport regime within this energy range (see Figs. 4 and 5). Indeed, as shown in the right panel of Fig. 4, the averaged conductance at those energy values remains very close to its maximum value of 1 G_0 (with G_0 the conductance quantum, $G_0 = 2e^2/h$).

This is also clear in the top panel of Fig. 5, where the mean free path l_e and the localization length ξ present values of a few microns. As it can be seen, $l_e \approx \xi$ for energies where there is just one propagating channel ($N_\perp$=1), whereas ξ increases with $N_\perp$ for higher energies (qualitatively consistent with the Thouless relationship $\xi \approx N_\perp l_e$).

We note that, however, the transport profiles and the values for l_e and ξ are very much dependent on the actual edge reconstruction [9]. This leads to very different behaviours of these typical transport lengths for each defect type. The values for l_e and ξ as a function of energy and length are plotted in Fig. 5 for a selection of edge defects. All the calculations have been performed using the tuned TB Hamiltonians parametrized according to the *ab initio* results as explained in section 2.

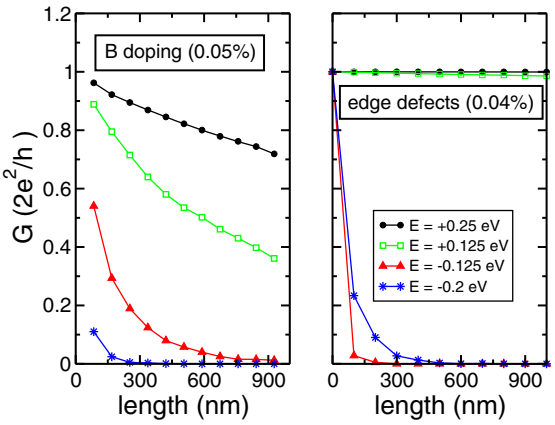

Figure 4 Conductance as a function of the length for the 35-aGNR at a (left) doping rate of 0.05% and (right) edge defect density of 0.04% for several fixed lengths.

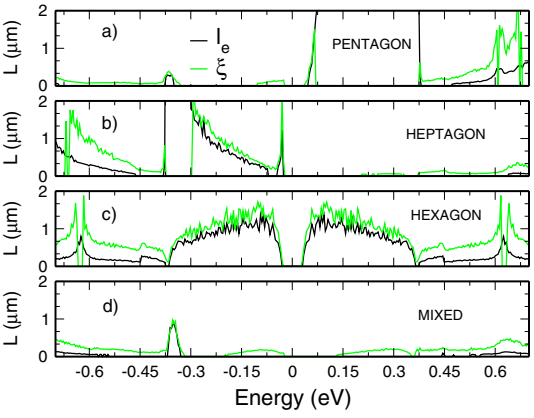

Figure 5 Elastic mean free path l_e and localization length ξ as a function of the energy for the 35-aGNR at a defect density of 0.04% and different types of defects. From top to bottom: pentagon-like, heptagon-like, hexagon-like, and mixed of the former three defects.

5 Conclusions We have analyzed the electronic transport properties of disordered aGNRs and CNTs at the mesoscopic scale. Both chemical doping and edge defects have been considered by means of suitable TB Hamiltonians derived from first-principles calculations. CNTs appear to be more robust than aGNRs against doping-induced disorder, while aGNRs with a length up to a few μm remain within the quasiballistic regime for certain types of edge defects.

Acknowledgements B.B. is indebted to the Juan de la Cierva program of the Spanish MICINN for financial support. A.C. acknowledges support from CARNOT graphene from LETI.

References

[1] J.-Ch. Charlier, X. Blase, and S. Roche, Rev. Mod. Phys. **79**, 677 (2007).
[2] A. Cresti, N. Nemec, B. Biel, G. Niebler, F. Triozon, G. Cuniberti, and S. Roche, Nano Research **1**, 361 (2008).
[3] B. Biel, F. Triozon, X. Blase, and S. Roche, Nano Lett. **9**, 2725 (2009).
[4] B. Biel, X. Blase, F. Triozon, and S. Roche, Phys. Rev. Lett. **102**, 096803 (2009).
[5] K. Nakada et al., Phys. Rev. B **54**, 17 954 (1996); K. Wakabayashi, Phys. Rev. B **64**, 125428 (2001). K. Sasaki, S. Saito, and R. Saito, Appl. Phys. Lett. **88**, 113110 (2006).
[6] Y.-W. Son, M.L. Cohen, and S.G. Louie, Phys.Rev.Lett. **97**, 216803 (2006); V. Barone, O. Hod, and G. E. Scuseria, Nano Lett. **6**, 2748 (2006); C.T. White, J. Li, D. Gunlycke, and J. W. Mintmire, Nano Lett. **7**, 825 (2007).
[7] D. Sánchez-Portal, P. Ordejon, E. Artacho, and J.M. Soler, Int. J. Quantum. Chem. **65**, 453 (1997).
[8] R. Avriller, S. Latil, F. Triozon, X. Blase, S. Roche, Phys. Rev. B. **74**, 121406(R) (2006).
[9] S.M.-M. Dubois, A. Lopez-Bezanilla, A. Cresti, B. Biel, F. Triozon, J.-Ch. Charlier, and S. Roche, submitted.
[10] Ch. Adessi, X. Blase, and S. Roche, Phys. Rev. B. **73**, 125414 (2006).
[11] R. Avriller, S. Roche, F. Triozon, X. Blase, and S. Latil, Mod. Phys. Lett. B. **21**, 1955 (2007).
[12] H.J. Choi, J. Ihm, S.G. Louie, and M.L. Cohen, Phys. Rev. Lett. **84**, 2917 (2000).
[13] Ch. Adessi, unpublished.
[14] D.A. Areshkin, D. Gunlycke, and C.T. White, Nano Lett. **7**, 204 (2007); D. Gunlycke, D.A. Areshkin, and C.T. White, Appl. Phys. Lett. **90**, 142104 (2007); D. Gunlycke and C.T. White, Phys. Rev. B **77**, 115116 (2008).
[15] D. Querlioz et al., Appl. Phys. Lett. **92**, 042108 (2008).
[16] M. Evaldsson, I.V. Zozoulenko, H. Xu, and T. Heinzel, Phys. Rev. B **78**, 161407(R) (2008).
[17] A. Cresti and S. Roche, Phys. Rev. B **79**, 233404 (2009).
[18] A. Cresti and S. Roche, New J. Phys. **11**, 095004 (2009).
[19] P. Koskinen, S. Malola, and H. Häkkinen, Phys. Rev. Lett. **101**, 115502 (2008).
[20] The drastic drop of the conductance close to the subband onset in Figs. 2 and 4 is a consequence of the enhanced scattering due to the larger density of states at the van Hove's singularities. It is enhanced with increasing disorder, and it is absent in the single-dopant calculation since in this case there are no disorder-induced multiple scattering effects.